



# Adaptive Evolution of *Rhodospiridium toruloides* with Ultra-centrifugal Fractionation Leads to a High Microbial Lipid Production using Crude Glycerol Feedstock

Xinru Wang<sup>1</sup> · Qi Liu<sup>1</sup> · Bin Zhang<sup>1</sup> · Jie Bao<sup>1</sup>

Received: 19 June 2025 / Accepted: 23 September 2025

© The Author(s), under exclusive licence to Springer Science+Business Media, LLC, part of Springer Nature 2025

## Abstract

In situ reintegration of crude glycerol into lipid feedstock can increase the production efficiency and environmental tolerance for the biodiesel industry. In this study, a wild oleaginous yeast *Rhodospiridium toruloides* CGMCC 2.1389 was selected for its high cell growth and lipid accumulation in crude glycerol. Ultra-centrifugal fractionation was applied in a long-term adaptive evolution, and a stable *R. toruloides* XR20 strain was finally obtained. The lipid content and titer of the *R. toruloides* XR20 strain in flask increased by 100.1% and 75.8% compared with the parental strain. Record-breaking lipid titers using crude glycerol by *R. toruloides* XR20 were achieved by batch and fed-batch fermentation, reaching  $24.5 \pm 0.5$  g/L and  $42.5 \pm 0.8$  g/L, respectively. *R. toruloides* XR20 showed enlarged intracellular space, higher intracellular NADPH, and acetyl-CoA contents compared with the parental strain. The changes in the expression levels of the key genes favored lipid synthesis in *R. toruloides* XR20. This study constructed a robust high lipid-producing *R. toruloides* on crude glycerol, contributing to a glycerol-free biodiesel production process.

**Keywords** Biodiesel · Crude glycerol · *Rhodospiridium toruloides* · Microbial lipid · Ultra-centrifugal fractionation

## Introduction

Crude glycerol is the major byproduct of biodiesel industrially generated in the transesterification of lipids with alcohols, with the yield of 10% of the biodiesel product [1]. The booming biodiesel market resulted in an overproduction of crude glycerol, with an annual output of 7.66 million tons, which is much higher than the market demand for glycerol [2]. Crude glycerol contains a variety of impurities, including alkaline catalysts, alcohols, free

---

✉ Bin Zhang  
binzh@ecust.edu.cn

✉ Jie Bao  
jbao@ecust.edu.cn

<sup>1</sup> State Key Laboratory of Bioreactor Engineering, East China University of Science and Technology, 130 Meilong Road, Shanghai 200237, China

fatty acids, soap, and salts [3]. Refining crude glycerol into pure glycerol for pharmaceutical, cosmetic, or food use is very costly [1, 4, 5]. On the other hand, in situ utilization of crude glycerol into lipids by oleaginous microorganisms for biodiesel production presents a promising strategy to develop a green process and eliminate the need for energy-intensive glycerol refining [2, 6].

Oleaginous yeasts are the major cell factories for the production of microbial lipid using glycerol [7]. Besides the process intensifications such as purification of crude glycerol [8], optimization of medium composition [9], fed-batch or two-stage fermentations [10, 11], and additives use [12, 13], the construction of high lipid-producing oleaginous yeast also plays a crucial role for the efficient lipid production from crude glycerol. Qiao et al. [14] simultaneously overexpressed stearoyl-CoA desaturase (SCD), diacylglyceride acyltransferase (DGA1), and acetyl-CoA carboxylase (ACC1) genes in *Y. lipolytica*, resulting in faster cell growth and higher lipid production from crude glycerol. In addition to rational metabolic engineering, adaptive laboratory evolution (ALE) is another innovative approach to generate desired microbial strains by culturing over multiple generations under a specific selection pressure [15]. Tsirigka et al. [16] conducted the adaptive evolution of *Y. lipolytica* on crude glycerol for 520 generations; however, the lipid production performance only increased by 1.1 to 1.6-fold compared to the parental strains.

Lipids (0.88–0.90 g/mL) have relatively lower density compared with broth [17]. Therefore, the density of individual cells tends to decrease as the lipid content increases, making it possible to screen high-lipid content mutants based on the differences in cell density [18]. Even simple gravimetric enrichment can facilitate the screening of high-lipid accumulating microalgae mutants [19]. Our previous study strengthened the screening efficiency by performing ultra-centrifugation on fermentation broth. An efficient adaptive evolution method coupled with ultra-centrifugal fractionation was thus proposed and verified to obtain the high-lipid-containing *Trichosporon cutaneum* mutants, which had 5–10 times greater lipid production than the parental strain [20, 21]. This method was based on the principle of density gradient centrifugation for separating different cell types; the higher lipid content mutants with lower density can be isolated in the upper layer of the broth [17, 22]. This adaptive evolution method with ultra-centrifugal fractionation was further applied to develop the high lipid-producing oleaginous yeast cells using crude glycerol as carbohydrate feedstock in this study. *Rhodospiridium toruloides* was selected due to its higher tolerance to crude glycerol. The obtained *R. toruloides* strain showed a significantly improved lipid production using crude glycerol. This study efficiently achieved the reintegration of crude glycerol into microbial lipid through targeted adaptive laboratory evolution of *R. toruloides*, providing a solution for the glycerol-free biodiesel industry.

## Materials and Methods

### Feedstock

The crude glycerol was kindly provided by Longyan New Energy Co., Longyan, Fujian, China. The crude glycerol (pH 5.6) contained ~853 g/L pure glycerol and ~110 g/L fatty acid methyl esters. The composition of fatty acids in the methyl esters included 2.0% (w/w) myristic acid (C14:0), 26.4% (w/w) palmitic acid (C16:0), 3.0% (w/w) palmitoleic acid (C16:1), 8.1% (w/w) stearic acid (C18:0), 39.4% (w/w) oleic acid (C18:1), and 22.1%

(w/w) linoleic acid (C18:2). The main cations concentration in crude glycerol including K, Na, Ca, Mg, P, S was 1.5 g/L, 2.5 g/L, 2.7 g/L, 0.2 g/L, 0.3 g/L, and 0.5 g/L.

## Strains and Medium

Three typical oleaginous yeasts were used to evaluate the lipid production performance using crude glycerol, including *Trichosporon cutaneum* ACCC 20271, *Yarrowia lipolytica* DSM 3286, and *Rhodospiridium toruloides* CGMCC 2.1389. YPD medium consisting of 20.0 g/L glucose, 20.0 g/L peptone, and 10.0 g/L yeast extract was used to activate the yeast strains. The lipid fermentation medium contained 95 g/L crude glycerol, equivalent to ~80 g/L pure glycerol, 1.0 g/L  $\text{MgSO}_4 \cdot 7\text{H}_2\text{O}$ , 0.42 g/L corn steep liquor, 1.25 g/L  $(\text{NH}_4)_2\text{SO}_4$ , and 2.0 g/L  $\text{KH}_2\text{PO}_4$ . The medium used for adaptive evolution contained 100.0 g/L crude glycerol, 1.0 g/L  $\text{MgSO}_4 \cdot 7\text{H}_2\text{O}$ , 1.0 g/L corn steep liquor, 1.0 g/L  $(\text{NH}_4)_2\text{SO}_4$ , and 1.0 g/L  $\text{KH}_2\text{PO}_4$ .

## Adaptive Evolution with Ultra-centrifugal Fractionation

*R. toruloides* CGMCC 2.1389 was cultured in YPD medium at 30 °C, 200 rpm for 24 h as the seed. Then the broth was inoculated into the medium used for adaptive evolution at a 10% (v/v) inoculation ratio. The culture was conducted at 30 °C, 200 rpm for 144 h. Then 20 mL of the broth was taken into a 50-mL sterilized centrifuge tube and centrifuged for 5 min (Avanti J-26 XP, Beckman Coulter, Brea, USA). After the centrifugation, the cell mass aggregated into the upper layer of the broth was dispersed by the pipette, and 5 mL of the supernatant broth was taken as the seed for the next round of culture. The centrifugation force gradually increased from 45,000 g to 53,000 g (the ceiling of the centrifugal machine) during the successive 20 transfers (total 120 days).

## Cell Morphology

The cell morphology was observed by optical microscope (HT2000 CN, Olympus, Japan) and field emission scanning electron microscope (FESEM) (JSM-IT800, JEOL, Japan) according to the previous protocols [21]. The cell length and diameter were analyzed by the software Image J (1.46r version). The cell volume was calculated according to the ellipsoidal volume calculation formula [20]. More than 50 cells were selected to calculate cell volume, excluding the immature cells and dividing cells.

## Lipid Production in Flasks and 3 L Fermenter using Crude Glycerol

The key medium ingredients for lipid fermentation using crude glycerol were optimized in flasks, including the initial crude glycerol concentration (80–140 g/L), initial  $\text{KH}_2\text{PO}_4$  concentration (0–3 g/L), and the ratio of corn steep liquor to  $(\text{NH}_4)_2\text{SO}_4$  (0–0.75). The fermentation in flasks was conducted at 30 °C, 200 rpm for 144 h. For the batch fermentation in a 3 L fermenter, the conditions were set at 30 °C, 1.0 vvm, 600 rpm for 144 h. The working volume was 1.0 L. The fermentation pH was controlled at 5.6 by automatically adding 3 M HCl and 3 M NaOH solution. A total of 5 mL of defoaming agent (GLT-700, Grade Inc., Jiangsu) was added before the fermentation. For the fed-batch fermentation, a total of three feedings were

carried out on the 3rd, 6th, and 8th day, respectively, at which time the residual glycerol concentration increased from ~40 g/L to ~80 g/L.

## RNA Extraction and RT-qPCR

*R. toruloides* strains were cultured in crude glycerol-contained medium for 24 h. The cell mass was collected and used for RNA extraction (Trizol reagent, RNAiso Plus, TAKARA) according to the instructions. Reverse transcription reactions and real-time qPCR (RT-qPCR) were conducted using Master Mix with gDNA Remover kit (Toyobo) and SYBR Green Real-time PCR Master Mix kit (Toyobo). The actin gene was selected as an internal control to standardize variations in total RNA amounts. The relative transcription level of the genes was calculated using  $2^{-\Delta\Delta C_t}$ . The GenBank accession number of the genome of *R. toruloides* was ALAU000000000 [23]. The primers used for RT-qPCR were shown in Table S1 (see supplementary materials).

## Analytical Methods

Glycerol concentration was measured by HPLC method. The Shimadzu HPLC system was equipped with an HPX-87 H column (Bio-rad Aminex) and RID-10A detector. The mobile phase was 5 mM H<sub>2</sub>SO<sub>4</sub> at the flow rate of 0.6 mL/min.

The colony-forming units (CFU) were determined by diluting the broth with the sterilized water, spreading on YPD agar medium, and culturing for 48 h.

The cell concentration (cells/mL) was counted using a Hemocytometer. Each sample was counted in triplicate, and the average value was taken. If the cell density was too high, the cell suspension was appropriately diluted before counting.

The intracellular acetyl-CoA content was measured by the ELISA Kit (A-CoA, COIBO, Shanghai). The intracellular NADPH was measured using the Assay Kit purchased from Beyotime Biotechnology (Shanghai) Co., Shanghai, China. The main cell wall components' contents, including glucan, mannan, and chitin, were measured by reported methods [24, 25].

Dry cell weight (DCW) was measured by the differential weighting method. The lipid was extracted using the methanol-chloroform method [26]. The 500  $\mu$ L of extracted lipid was added into 5 mL of the mixed reagent (the ratio of boron trifluoride to methanol is 1:6) in the flask. The flask was equipped with a reflux condenser and heated in an oil bath at 80 °C, 400 rpm for 40 min. Then 6 mL of deionized water and 4 mL of n-hexane were added into the flask. The mixture was shaken, and the upper layer was extracted for the analysis of fatty acids of the lipid by gas chromatography-mass spectrometry (GC-MS).

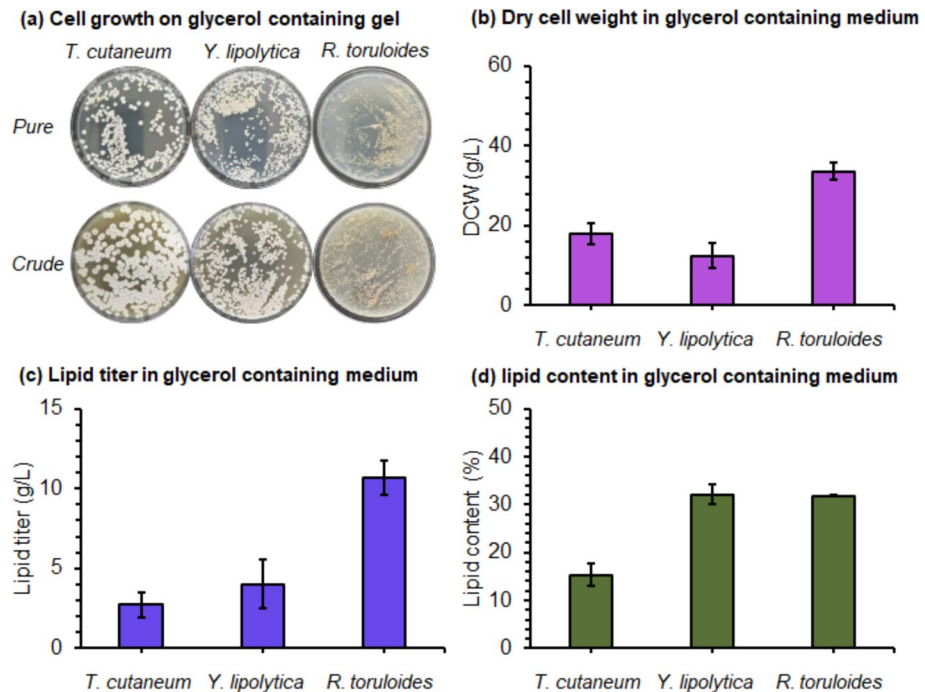
The conditions of GC-MS were as follows: the injection temperature of 280 °C, injection volume of 0.4  $\mu$ L, helium as the carrier gas at a flow rate of 1 mL/min, an Agilent 19091 J-433 column (30 m  $\times$  250  $\mu$ m  $\times$  0.25  $\mu$ m). The flame ionization detector was set at 120 °C with the program that held at 80 °C for 3 min, then increased to 280 °C at a rate of 16 °C/min and held for 8 min. The analysis software was NIST MS Search 2.0.

## Results

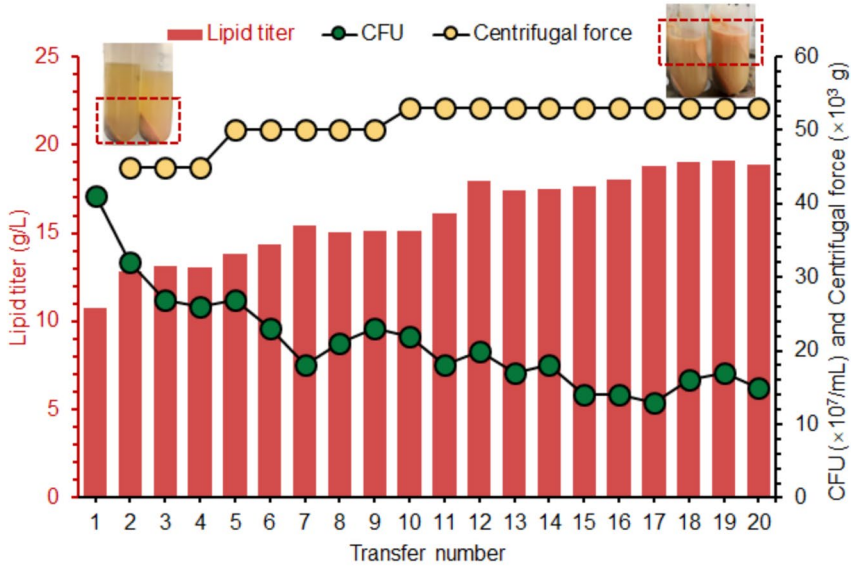
### Adaptive Evolution of *R. toruloides* CGMCC 2.1389 with Ultra-centrifugal Fractionation in Crude Glycerol Medium

Three typical oleaginous yeast strains, *T. cutaneum* ACCC 20271, *Y. lipolytica* DSM 3286 and *R. toruloides* CGMCC 2.1389, were chosen and cultured on the agar plates containing 80 g/L pure glycerol or 95 g/L crude glycerol (glycerol content 85.3%, w/v) (Fig. 1a). All the three oleaginous yeasts grew well on pure glycerol and crude glycerol plates. The flask test using crude glycerol showed that *R. toruloides* had the higher cell growth ( $33.5 \pm 2.1$  g/L dry cell mass) and lipid accumulation ( $10.7 \pm 1.1$  g/L) (Fig. 1b and c). These results indicate that the wild *R. toruloides* CGMCC 2.1389 has the greater potential for lipid production from crude glycerol compared to the other two oleaginous strains, but the relatively low lipid content of *R. toruloides* limited the lipid accumulation (Fig. 1d).

Adaptive evolution with ultra-centrifugal fractionation was applied to improve the lipid production of *R. toruloides* on crude glycerol (Fig. 2a). After 144 h of culture, 20 mL of the broth was taken and centrifuged for 5 min under the centrifugal force from 45,000 g to 53,000 g (Fig. 2b). The upper layer that contained lighter cells with higher lipid content was pipetted as the seed for the next round of culture. A series of cultures, centrifugations, and transfers were conducted for 20 times. The lipid titer of *R. toruloides* from



**Fig. 1** Oleaginous yeast evaluation for lipid production using crude glycerol. (a) Cell growth on glycerol-containing plates at 30 °C, 48 h; (b) Dry cell weight (DCW) after 6 days' culture in liquid medium containing 95 g/L of crude glycerol at 30 °C, 200 rpm. (c) Lipid titers after 6 days' culture in liquid medium containing 95 g/L of crude glycerol. (d) Intracellular lipid content

**(a) The schematic diagram of adaptive evolution with centrifugation and fractionation****(b) Adaptive evolution of *R. toruloides* under the stress of ultra-centrifugation and fractionation**

**Fig. 2** Adaptive evolution of *R. toruloides* with ultra-centrifugal fractionation in crude glycerol. **(a)** The schematic diagram of adaptive evolution with centrifugal fractionation. **(b)** The changes in lipid titer, CFU, cells distribution of *R. toruloides* during the adaptive evolution with ultra-centrifugal fractionation

crude glycerol increased from 10.7 g/L to 18.9 g/L, while the CFU values decreased from  $4.1 \times 10^8$  to  $1.5 \times 10^8$ . A large number of cells were suspended in the upper layer of the broth after the centrifugation of the finally obtained *R. toruloides*. In contrast, almost all the cells of the parental strain after centrifugation were deposited at the bottom of the tube, and the supernatant was relatively clear. The final obtained cells were spread on PDA agar plates, and a single colony was isolated as *R. toruloides* XR20.

### Characterizations of *R. toruloides* XR20

The cell volume of *R. toruloides* gradually enlarged along with the adaptive evolution from the observation by optical microscope (Fig. 3a). The observation by field emission scanning electron microscope (FESEM) further showed that *R. toruloides* XR20 presented larger cell volume with longer cell diameters compared to the parental strain (Fig. 3b). The average cell volume of *R. toruloides* XR20 calculated according to SEM images was 181.0

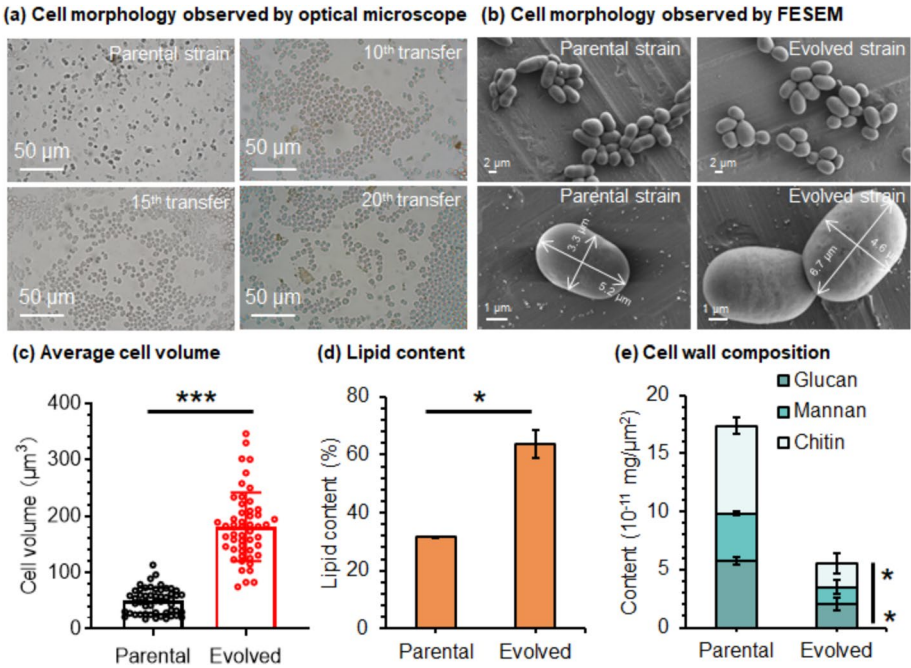


**Fig. 3** Characterizations of *R. toruloides* XR20 compared to the parental strain. **(a)** The cell morphology observed by optical microscope before centrifugation. **(b)** The cell morphology observed by FESEM after 72 h of culture. **(c)** Cell volume calculated according to the images of FESEM. The mean value of cell volume of evolved *R. toruloides* XR20 is significantly higher than that of the parental group, as determined by *t*-test ( $P < 0.0001$ ). **(d)** The lipid content after 144 h of culture in crude glycerol-contained medium. **(e)** The contents of main cell wall components. Variations were considered statistically significant at \*  $P < 0.05$ , \*\*  $P < 0.01$ , and \*\*\*  $P < 0.001$ . FESEM, field emission scanning electron microscope

$\mu\text{m}^3$ , which was 3.6 times larger than that of the parental cell ( $49.7 \mu\text{m}^3$ ) (Fig. 3c). The lipid content of *R. toruloides* XR20 in crude glycerol medium reached  $63.6 \pm 4.7\%$  (w/w), which was twice as much as that of the parental strain (Fig. 3d). The increased cell volume reduced the thickness of the cell wall in *R. toruloides* XR20. The contents of main components of the yeast cell wall including glucan, mannan, and chitin [27], decreased by 65.5%, 62.8%, and 73.5% in *R. toruloides* XR20 compared to the parental strain (Fig. 3e).

NADPH and acetyl-CoA are important biosynthetic precursors of lipids [28]. The intracellular contents of NADPH and acetyl-CoA in *R. toruloides* XR20 increased by 15.2%–42.2% and 68.8%–168.8%, respectively, compared with those of the parental strain (Figs. 4a, 3b). In typical oleaginous yeast, NADPH is provided in the conversion of malate into pyruvate by malic enzyme (ME) in the cytosol [29]. The transcriptional level of ME in evolved *R. toruloides* XR20 was up-regulated by  $4.64 \pm 0.27$  (Fig. 4c). The up-regulation of NADP<sup>+</sup>-dependent isocitrate dehydrogenase (IDH) ( $5.66 \pm 0.22$ ) also contributed to the regeneration of NADPH in *R. toruloides* XR20 (Fig. 4c). ATP-dependent citrate lyase is generally thought to play a critical role in lipid biosynthesis by catalyzing the reaction of citrate into acetyl-CoA [30]. However, the expression level of ACL ( $0.81 \pm 0.19$ ) in evolved *R. toruloides* XR20 was significantly down-regulated. The up-regulations of succinate dehydrogenase (SDH), fumarate hydratase (FH), and malate dehydrogenase (MDH) in the TCA cycle promoted the production of pyruvate, which was subsequently converted into

**Fig. 4** Comparisons of NADPH, acetyl-CoA, and gene expression levels in central glycerol metabolism of lipid biosynthesis between the parental *R. toruloides* and *R. toruloides* XR20. **(a)** Intracellular NADPH content at 24 h, 48 h, and 72 h. **(b)** Intracellular acetyl-CoA content at 24 h, 48 h, and 72 h. Variations were considered statistically significant at \*  $P < 0.05$ . NADPH, nicotinamide adenine dinucleotide phosphate. **(c)** Transcriptional analysis of the genes involved in central glycerol metabolism of lipid biosynthesis compared to the parental strain. The samples were collected after cultured in 95 g/L crude glycerol medium for 24 h. The gene expression levels were normalized against the parental strain. Each RT-qPCR was performed at least three times. ACL, ATP-dependent citrate lyase; ACC, acetyl-CoA carboxylase; ACO, aconitase; CS, citrate synthase; DAK1, dihydroxyacetone kinase; DGAT, diacylglycerol acyl-transferase; ELO, fatty acid elongase; ENO, enolase; FAD1/2, fatty acid desaturase 1/2; FAS1/FAS2, fatty acid synthase 1/2; FH, fumarate hydratase; GAPD, glyceraldehyde-3-phosphate dehydrogenase; GCY1, glycerol kinase 1; GPAT, glycerol-3-phosphate acyltransferase; GPD, glycerol-3-phosphate dehydrogenase; GPD1/GPD2, glycerol-3-phosphate dehydrogenase 1/2; GUP, glycerol uptake protein; GUT1/GUT2, glycerol utilization protein 1/2; ICL, isocitrate lyase; IDH, NADP<sup>+</sup>-dependent isocitrate dehydrogenase; LPAT, lysophosphatidic acid acyltransferase; MDH, malate dehydrogenase; ME, malic enzyme; MLS, malate synthase; PAP, phosphatidic acid phosphatase; PC, pyruvate carboxylase; PDHA/PDHB, pyruvate dehydrogenase E1  $\alpha/\beta$  subunit; PGK, phosphoglycerate kinase; PGM, phosphoglycerate mutase; PYK, pyruvate kinase; SCS, succinyl-CoA synthetase; SDH, succinate dehydrogenase; TPI, triose phosphate isomerase;  $\alpha$ KDH,  $\alpha$ -ketoglutarate dehydrogenase

acetyl-CoA by pyruvate dehydrogenase (PDH). The result of transcriptional analysis indicated that the increased content of acetyl-CoA in evolved *R. toruloides* XR20 is attributed to the higher expression levels of some genes in the TCA cycle rather than the high expression of AC, which is similar to the study reported by Zhao et al. in *Rhodotorula glutinis* [31]. The genes encoding phosphatidic acid phosphatase (PAP) and diacylglycerol acyltransferase (DGAT) were up-regulated by  $7.52 \pm 0.97$  and  $4.10 \pm 0.38$ , which also facilitated the triacylglycerol biosynthesis. In short, the adaptive evolution with ultra-centrifugal fractionation changed the cell morphology and metabolic flux of *R. toruloides*, which was favorable for the accumulation of lipid from crude glycerol.

### Lipid Production from Crude Glycerol by *R. toruloides* XR20

The key conditions for lipid production by *R. toruloides* from crude glycerol were optimized, including the initial crude glycerol concentration, initial  $\text{KH}_2\text{PO}_4$  concentration, and the ratio of corn steep liquor (CSL) to  $(\text{NH}_4)_2\text{SO}_4$  (Fig. 5). The high crude glycerol concentration in medium led to a higher osmotic pressure and higher inhibitors [13]. The results showed that the highest lipid titer was obtained at 100 g/L initial crude glycerol concentration, which reached  $15.6 \pm 0.9$  g/L (Fig. 5a). The adequate limitation of phosphorus is necessary to promote lipid accumulation in *R. toruloides* [32, 33]. The results showed that despite the low phosphorous content in crude glycerol ( $0.3 \pm 0.1$  g/L), the lipid titer increased to  $18.6 \pm 0.5$  g/L after the supplementation with 2 g/L  $\text{KH}_2\text{PO}_4$  (Fig. 5b). The cheap corn steep liquor (CSL) instead of yeast extract was used as a complex nitrogen source for lipid production from crude glycerol (Fig. 5c). The results showed that the highest lipid titer reached  $20.0 \pm 0.4$  g/L when the ratio of CSL to  $(\text{NH}_4)_2\text{SO}_4$  was 0.25, which was equivalent to 0.42 g/L CSL (74.4% solid content, w/w) and 1.25 g/L  $(\text{NH}_4)_2\text{SO}_4$ .

The batch fermentation was conducted in a 3 L fermenter using the optimized medium ingredients. The lipid titer of the parental strain increased to  $17.4 \pm 0.1$  g/L from 100 g/L crude glycerol. The lipid titer of *R. toruloides* XR20 reached  $24.5 \pm 0.5$  g/L, which was 40.8% higher than that of the parental strain (Fig. 6a). The lipid yield and productivity of *R. toruloides* XR20 reached 0.32 g/g consumed glycerol and 4.1 g/L/d. Almost all the glycerol (less than 5 g/L) was consumed by the parental *R. toruloides* and *R. toruloides* XR20

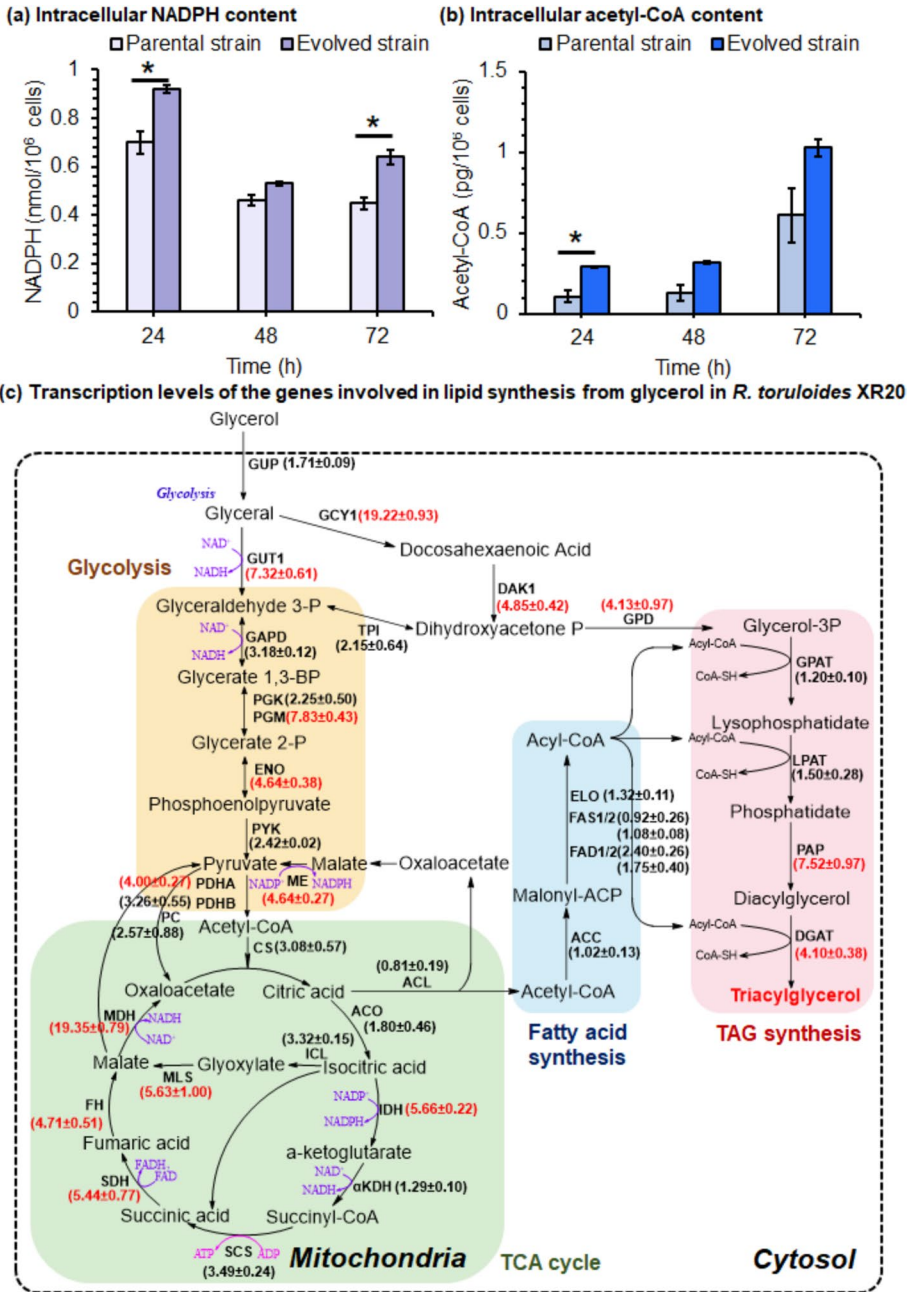


(Fig. 6b). *R. toruloides* was reported to have the capability to utilize a broad substrate [34]. Almost no fatty acid methyl esters were detected in the broth after 144 h fermentation (Fig. 6c). The parental strain showed higher cell growth, but the CFU values increased within 48 h and sharply decreased from 48 to 144 h (Fig. 6d), indicating that the autolysis of a large number of cells occurred in the late stage of fermentation. The CFU values of *R.*

**Fig. 5** Optimizations of key fermentation conditions. **(a)** Initial glycerol concentration. The crude glycerol concentrations of 80, 100, 120, 140 g/L are equivalent to the initial glycerol concentrations of 68.2, 85.3, 102.4, 119.4 g/L. The nitrogen source included 1.0 g/L corn steep liquor and 1.0 g/L  $(\text{NH}_4)_2\text{SO}_4$ . **(b)** Initial  $\text{KH}_2\text{PO}_4$  concentration. **(c)** Ratio of corn steep liquor (CSL) to  $(\text{NH}_4)_2\text{SO}_4$ . The concentrations of CSL and  $(\text{NH}_4)_2\text{SO}_4$  are 0, 0.42, 1.0, 1.9 g/L and 1.4, 1.25, 1.0, 0.64 g/L, respectively, at the ratio of 0, 0.25, 0.5 and 0.75. The water content of CSL was 74.4% (w/w)

*toruloides* XR20 increased consistently and exceeded those of the parental strain at 144 h, indicating that *R. toruloides* XR20 may have a longer cell cycle.

The fatty acids composition of the lipid produced from crude glycerol by *R. toruloides* XR20 was determined. The results showed that the lipid mainly consisted of C16 to C18 fatty acids, and the content of unsaturated fatty acids including oleic acid (C18:1) and linoleic acid (C18:2) was more than 57% (Fig. 6e). The greater content of monounsaturated fatty acid is favorable for the production of biodiesel by transesterification [35].

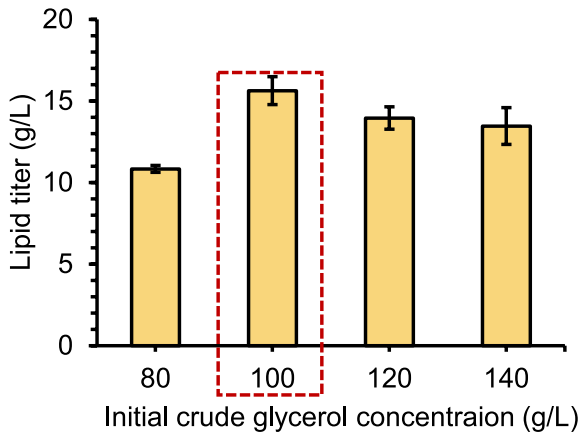
The highly concentrated crude glycerol is favorable for fed-batch fermentation to avoid high osmotic pressure and high viscosity and achieve high lipid titers [36]. The feeding was performed on the 3rd, 6th, and 8th day of the fermentation, respectively (Fig. 7, red arrows). A record-breaking lipid titer from crude glycerol by *R. toruloides* XR20 was achieved by fed-batch fermentation, reaching  $42.5 \pm 0.8$  g/L. The lipid yield and productivity of *R. toruloides* XR20 by fed-batch fermentation were only 0.24 g/g consumed glycerol and 3.9 g/L/d, which were lower than that by batch fermentation, but greater cell growth (CFU) was achieved.

## Discussion

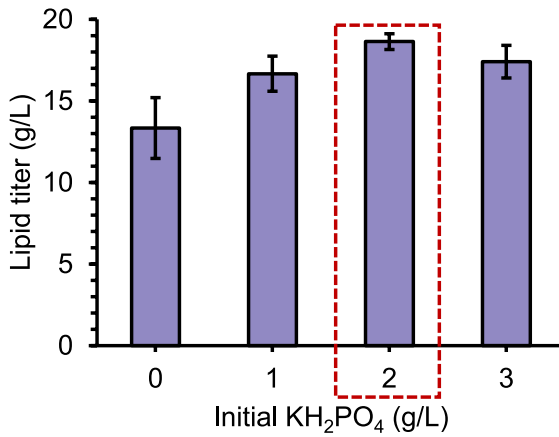
Biodiesel, ranking as the second most extensively produced liquid biofuel following bioethanol worldwide [37]. The boom in the biodiesel market would lead to the overproduction of by-product crude glycerol. It is important to develop the method for the proper disposal of crude glycerol. Otherwise, crude glycerol would become a barrier for the sustainable production of biodiesel and threaten the environmental gains from replacing fossil fuels [1]. However, the refining of crude glycerol into pure glycerol is an expensive process. The direct application of crude glycerol as fuel or a fuel additive remains challenging due to the requirement for equipment modifications and additional fuel preparation steps [4, 5].

In-situ reintegration of crude glycerol into biodiesel production by oleaginous yeast stands out as a promising strategy. Despite the availability of advanced metabolic regulation tools, most of the existing research neglected to engineer a robust high lipid-producing yeast on crude glycerol. This study applied an adaptive evolution with ultracentrifugal fractionation method to develop high lipid-producing *R. toruloides* on crude glycerol. The ultracentrifugal fractionation was based on the principle of density gradient centrifugation, an approach that has been widely employed for separating diverse cell types, sub-cellular compartments, and macromolecular complexes according to their differential buoyant densities [18, 38]. The cells with higher lipid content generally exhibit lower cell density. The density gradient centrifugation method thus had been developed for isolating high lipid content mutants. By combining density gradient centrifugation and Nile red spectrofluorometry, Bracero et al. isolated high-lipid containing *Chlorella* sp. mutants [39]. In other studies, *Yarrowia lipolytica* or *Lipomyces starkeyi* were firstly treated by ethyl methanesulfonate to construct mutant libraries [22, 40]. Subsequently, after 3–5 rounds of density gradient centrifugation screening

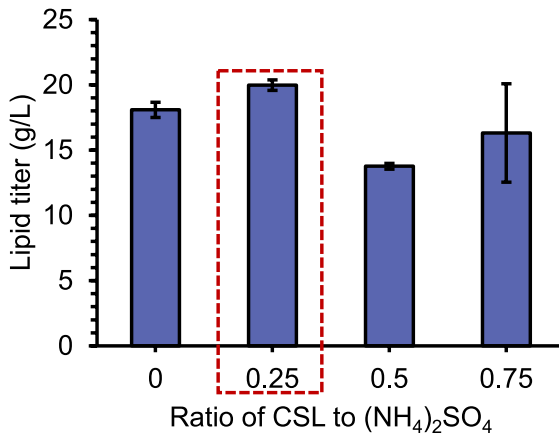
**(a) Optimization of initial crude glycerol concentration**

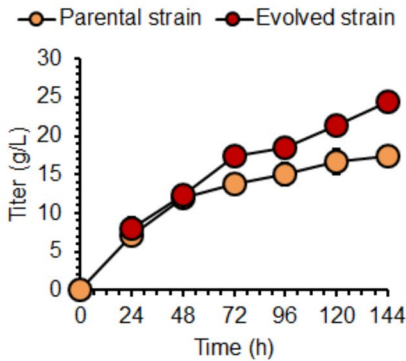
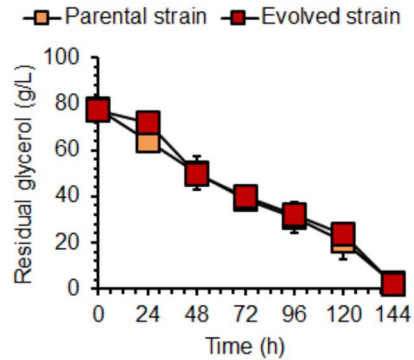
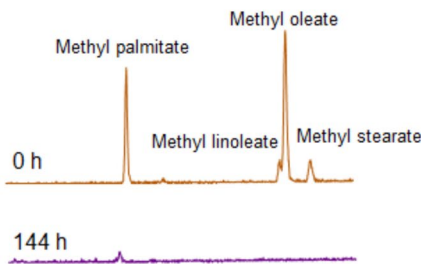
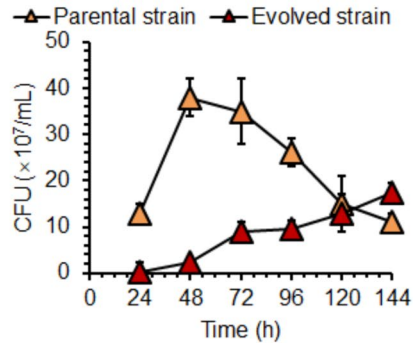
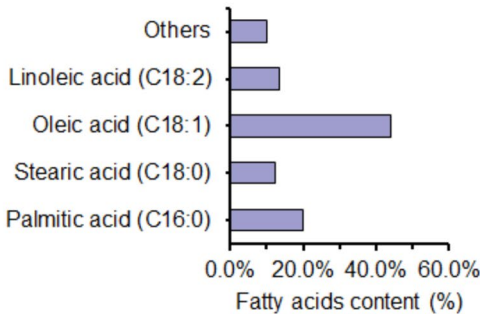


**(b) Optimization of  $\text{KH}_2\text{PO}_4$  concentration**



**(c) Optimization of the ratio of CSL to  $(\text{NH}_4)_2\text{SO}_4$**



**(a) Lipid titer in batch fermentation****(b) Residual glycerol in batch fermentation****(c) GC-MS analysis of fermentation broth****(d) CFU in batch fermentation****(e) Fatty acids composition of lipids**

**Fig. 6** Batch fermentation using crude glycerol by *R. toruloides*. **(a)** Lipid titer. **(b)** Residual glycerol. **(c)** GC-MS analysis of fermentation broth at 0 h and 144 h. **(d)** Colony-forming unit (CFU). **(e)** The fatty acids profile of the lipid produced from crude glycerol by *R. toruloides* XR20

(100–5000 g) and culture, the lipid titer of the obtained mutants was approximately 1.5 times that of the parental strains. In this study, the centrifugal force was further strengthened up to 53,000 g, enhancing the screening efficiency and significantly improving the lipid accumulation of *R. toruloides* mutant using crude glycerol. The lipid titer, productivity, and yield using crude glycerol by *R. toruloides* XR20 were compared with the

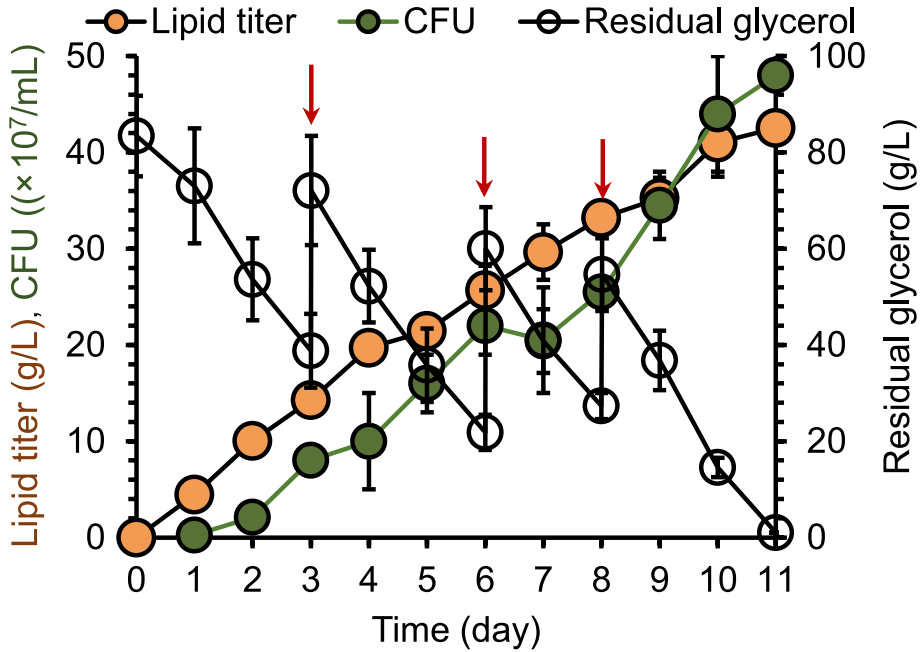


**Fig. 7** Fed-batch fermentation using crude glycerol by *R. toruloides* XR20. A total of three-time feedings was carried out on the 3rd, 6th, and 8th day, respectively, at which time the residual glycerol concentration increased from ~40 g/L to ~80 g/L

**Table 1** Lipid production performances by *Rhodotorula* species using crude glycerol

Strain	Mode	DCW (g/L)	Content (%)	Titer (g/L)	Source
<i>R. toruloides</i> AS 2.1389	Batch	26.7	~70	18.5	[41]
<i>R. mucilagenosa</i> I IPL32	Batch	20.0	~28	5.6	[42]
<i>R. graminis</i> DBVPG 4620	Batch	16.3	~53	8.6	[43]
<i>R. toruloides</i> XR20	Batch	37.5	65.3	24.5	This study
<i>R. glutinis</i> CICC 31596	Fed-batch	30.6	53.2	16.3	[44]
<i>R. fluvialis</i> DMKURK253	Fed-batch	39.1	79.4	27.8	[11]
<i>R. toruloides</i> DSM 4444	Fed-batch	37.4	51.3	19.2	[45]
<i>R. toruloides</i> Y4	Fed-batch	31.1	41.7	13	[46]
<i>R. paludigena</i> CM33	Fed-batch	46.3	37.7	17.4	[47]
<i>R. glutinis</i> BCRC 21418	Fed-batch	46.4	62.2	28.9	[48]
<i>R. toruloides</i> XR20	Fed-batch	56.7	74.9	42.5	This study

previously reported studies (Table 1). These key performance indicators of the batch and fed-batch fermentation in this study are advanced compared to the reported studies.

Density gradient centrifugation also can help identify genes significantly affecting lipid accumulation in yeast. After the transposon insertion mutagenesis in *Saccharomyces cerevisiae*, the lighter cells with higher lipid content were screened by density gradient

centrifugation. By analyzing the transposon insertion sites in mutants with elevated lipid content, Kmisaka et al. identified five key ORFs (open reading frames) influencing lipid accumulation [49]. However, this study only represents a preliminary investigation of lipid production using crude glycerol feedstock by adaptively evolved *R. toruloides*. Although we provided a plausible explanation about the phenomenon based on the reported studies, the following work should focus on mining vital mutant sites and gene targets using whole-genome resequencing and global transcriptomes in evolved *R. toruloides* XR20 for rational reverse metabolic engineering of *R. toruloides*.

Additionally, *R. toruloides* has been regarded as a promising source of natural colorants (i.e., carotenoids) [50]. We observed that the evolved *R. toruloides* XR20 strain exhibited a deeper red color and higher carotenoid accumulation compared to the parental strain, which may be owing to its increased lipid content providing more acetyl-CoA precursor and storage space for carotenoids [51]. The co-production of microbial lipid and carotenoids using crude glycerol would undoubtedly benefit this closed-loop biorefinery. The reduction of mannan and chitin in the yeast cell wall makes the cell wall more vulnerable to being broken down (Fig. 2e) [52], which will facilitate the downstream lipid and carotenoid recovery. Kumar et al. estimated that the biodiesel cost from crude glycerol was 0.77 \$/L [53]. A similar result was reported by Chen et al. that the biodiesel cost from crude glycerol and wastewater sludge was 0.63 \$/kg [9]. Compared to the current commercial biodiesel price of 1.27–1.54 \$/kg ([www.imarcgroup.com](http://www.imarcgroup.com)), the biodiesel production from crude glycerol is competitive. The raw material costs in lipid production from crude glycerol can be further controlled to improve the economic benefits [11]. Sun et al. reported that the nutrients in fermentation should be replaced by cheap alternatives [54]. Although the expensive yeast extract was replaced by cheap corn seep liquor in this study, a record-breaking lipid titer was still achieved from crude glycerol by the evolved *R. toruloides* XR20.

## Conclusions

This study employed the adaptive evolution with ultra-centrifugal fractionation to improve the lipid production of *R. toruloides* on crude glycerol. The lipid titer reached  $24.5 \pm 0.5$  g/L and  $42.5 \pm 0.8$  g/L by batch and fed-batch fermentation using crude glycerol with the optimized cheap ingredients. This adaptive evolution method significantly changed the cell morphology, cell structure, intracellular metabolite and genes expression levels in *R. toruloides* XR20, contributing to the enhancement of lipid production. *R. toruloides* XR20 strain can be served as an outstanding cell factory for in-situ reintegration of biodiesel-derived crude glycerol into lipid feedstock, benefiting the sustainability of biodiesel industrial.

**Supplementary Information** The online version contains supplementary material available at <https://doi.org/10.1007/s12010-025-05425-8>.

**Acknowledgements** The authors thank the kind donation of *R. toruloides* CGMCC 2.1389 by Prof. Zhao ZBK, Dalian Institute of Chemical Physics.

**Author Contribution** XW: Investigation, data curation, visualization, writing—original draft. QL: Data curation, formal analysis, writing—original draft. BZ: Conceptualization, funding acquisition, writing—review & editing. JB: Supervision, project administration, writing—review & editing.

**Funding** This research was supported by the National Key R&D Program of China (2023YFA0914400), the National Natural Science Foundation of China (32301269), the Science and Technology Committee of

Shanghai Municipality (23YF1409900), and the Key Technology R&D Program of the Science and Technology Commission of Shanghai Municipality (25HC2820200).

**Data Availability** All data are available from the corresponding author on request.

## Declarations

**Ethical Approval and Consent to Participate** This article does not contain any studies with human participants or animals performed by any of the authors.

**Consent for Publication** All the authors hereby give their consent for publication.

**Competing interests** The authors declare no competing interests.

## References

1. Monteiro, M. R., Kugelmeier, C. L., Pinheiro, R. S., Batalha, M. O., & da Silva César, A. (2018). Glycerol from biodiesel production: Technological paths for sustainability. *Renewable And Sustainable Energy Reviews*, *88*, 109–122. <https://doi.org/10.1016/j.rser.2018.02.019>
2. Zhao, M., Wang, Y., Zhou, W., Zhou, W., & Gong, Z. (2023). Co-valorization of crude glycerol and low-cost substrates via oleaginous yeasts to micro-biodiesel: Status and outlook. *Renewable And Sustainable Energy Reviews*, *180*, Article 113303. <https://doi.org/10.1016/j.rser.2023.113303>
3. Yang, F., Hanna, M. A., & Sun, R. (2012). Value-added uses for crude glycerol-a byproduct of biodiesel production. *Biotechnology for Biofuels*, *5*, 13. <https://doi.org/10.1186/1754-6834-5-13>
4. Gupta, M., & Kumar, N. (2012). Scope and opportunities of using glycerol as an energy source. *Renewable and Sustainable Energy Reviews*, *16*, 4551–4556. <https://doi.org/10.1016/j.rser.2012.04.001>
5. Zhang, J., Wang, Y., Muldoon, V. L., & Deng, S. (2022). Crude glycerol and glycerol as fuels and fuel additives in combustion applications. *Renewable And Sustainable Energy Reviews*, *159*, Article 112206. <https://doi.org/10.1016/j.rser.2022.112206>
6. Sarantou, S., Stoforos, N. G., Kalantzi, O., & Papanikolaou, S. (2021). Biotechnological valorization of biodiesel-derived glycerol: Trials with the non-conventional yeasts *Yarrowia lipolytica* and *Rhodospiridium* sp. *Carbon Resources Conversion*, *4*, 61–75. <https://doi.org/10.1016/j.crcon.2020.12.006>
7. Chattopadhyay, A., Mitra, M., & Maiti, M. K. (2021). Recent advances in lipid metabolic engineering of oleaginous yeasts. *Biotechnology Advances*, *53*, Article 107722. <https://doi.org/10.1016/j.biotechadv.2021.107722>
8. Kumar, L. R., Yellapu, S. K., Tyagi, R. D., & Drogui, P. (2020). Purified crude glycerol by acid treatment allows to improve lipid productivity by *Yarrowia lipolytica* SKY7. *Process Biochemistry*, *96*, 165–173. <https://doi.org/10.1016/j.procbio.2020.06.010>
9. Chen, J., Zhang, X., & Tyagi, R. (2021). Impact of nitrogen on the industrial feasibility of biodiesel production from lipid accumulated in oleaginous yeast with wastewater sludge and crude glycerol. *Energy*, *217*, Article 119343. <https://doi.org/10.1016/j.energy.2020.119343>
10. Chen, J., Zhang, X., Yan, S., Tyagi, R. D., & Drogui, P. (2017). Lipid production from fed-batch fermentation of crude glycerol directed by the kinetic study of batch fermentations. *Fuel*, *209*, 1–9. <https://doi.org/10.1016/j.fuel.2017.07.070>
11. Polburee, P., & Limtong, S. (2020). Economical lipid production from crude glycerol using *Rhodospiridiobolus fluvialis* DMKU-RK253 in a two-stage cultivation under non-sterile conditions. *Biomass and Bioenergy*, *138*, Article 105597. <https://doi.org/10.1016/j.biombioe.2020.105597>
12. Kamal, R., Liu, Y., Li, Q., Huang, Q., Wang, Q., Yu, X., & Zhao, Z. K. (2020). Exogenous l-proline improved *Rhodospiridium toruloides* lipid production on crude glycerol. *Biotechnology for Biofuels*, *13*, 1. <https://doi.org/10.1186/s13068-020-01798-6>
13. Liu, L., Zong, M., Hu, Y., Li, N., Lou, W., & Wu, H. (2017). Efficient microbial oil production on crude glycerol by *Lipomyces starkeyi* AS 2.1560 and its kinetics. *Process Biochemistry*, *58*, 230–238. <https://doi.org/10.1016/j.procbio.2017.03.024>
14. Qiao, K., Imam Abidi, S. H., Liu, H., Zhang, H., Chakraborty, S., Watson, N., Kumaran Ajikumar, P., & Stephanopoulos, G. (2015). Engineering lipid overproduction in the oleaginous yeast *Yarrowia lipolytica*. *Metabolic Engineering*, *29*, 56–65. <https://doi.org/10.1016/j.ymben.2015.02.005>

15. Chen, C., Li, Y., Chen, X., Wang, Y., Ye, C., & Shi, T. (2024). Application of adaptive laboratory evolution for *Yarrowia lipolytica*: A comprehensive review. *Bioresource Technology*, 391, Article 129893. <https://doi.org/10.1016/j.biortech.2023.129893>
16. Tsirigka, A., Theodosiou, E., Patsios, S. I., Tsourekis, A., Andreadelli, A., Papa, E., Aggeli, A., Karabelas, A. J., & Makris, A. M. (2023). Novel evolved *Yarrowia lipolytica* strains for enhanced growth and lipid content under high concentrations of crude glycerol. *Microbial Cell Factories*, 22, 62. <https://doi.org/10.1186/s12934-023-02072-8>
17. Sung, Y. J., Choi, H. I., Lee, J. S., Hong, M. E., & Sim, S. J. (2019). Screening of oleaginous algal strains from *Chlamydomonas reinhardtii* mutant libraries via density gradient centrifugation. *Biotechnology and Bioengineering*, 116(12), 3179–3188. <https://doi.org/10.1002/bit.27149>
18. Eroglu, E., & Melis, A. (2008). Density equilibrium method for the quantitative and rapid in situ determination of lipid, hydrocarbon, or biopolymer content in microorganisms. *Biotechnology and Bioengineering*, 102, 1406–1415. <https://doi.org/10.1002/bit.22182>
19. Hassanpour, M., Abbasabadi, M., Ebrahimi, S., Hosseini, M., & Sheikhabaglou, A. (2015). Gravimetric enrichment of high lipid and starch accumulating microalgae. *Bioresource Technology*, 196, 17–21. <https://doi.org/10.1016/j.biortech.2015.07.046>
20. Liu, Q., Li, Y., Hou, W., Zhang, B., & Bao, J. (2023). Cellulase mediated stress triggers the mutations of oleaginous yeast *Trichosporon cutaneum* with super-large spindle morphology and high lipid accumulation. *Biotechnology Journal*, 18, Article e2300091. <https://doi.org/10.1002/biot.202300091>
21. Liu, Q., Lu, M., Jin, C., Hou, W., Zhao, L., & Bao, J. (2022). Ultra-centrifugation force in adaptive evolution changes the cell structure of oleaginous yeast *Trichosporon cutaneum* into a favorable space for lipid accumulation. *Biotechnology and Bioengineering*, 119, 1509–1521. <https://doi.org/10.1002/bit.28060>
22. Yamazaki, H., Kobayashi, S., Ebina, S., Abe, S., Ara, S., Shida, Y., Ogasawara, W., Yaoi, K., Araki, H., & Takaku, H. (2019). Highly selective isolation and characterization of *Lipomyces starkeyi* mutants with increased production of triacylglycerol. *Applied Microbiology and Biotechnology*, 103(15), 6297–6308. <https://doi.org/10.1007/s00253-019-09936-3>
23. Zhu, Z., Zhang, S., Liu, H., Shen, H., Lin, X., Yang, F., Zhou, Y. J., Jin, G., Ye, M., Zou, H., & Zhao, Z. K. (2012). A multi-omic map of the lipid-producing yeast *Rhodospiridium toruloides*. *Nature Communications*, 3, 1112. <https://doi.org/10.1038/ncomms2112>
24. Domer, J. E. (1971). Monosaccharide and chitin content of cell walls of *Histoplasma capsulatum* and *Blastomyces dermatitidis*. *Journal of Bacteriology*, 107(3), 870–877. <https://doi.org/10.1128/jb.107.3.870-877.1971>
25. Manners, D. J., Masson, A. J., Patterson, J. C., Björndal, H., & Lindberg, B. (1973). The structure of a  $\beta$ -(1→6)-d-glucan from yeast cell walls. *Biochemical Journal*, 135, 31–36. <https://doi.org/10.1042/bj1350031>
26. Folch, J., Lees, M., & Stanley, G. H. S. (1957). A simple method for the isolation and purification of total lipides from animal tissues. *Journal of Biological Chemistry*, 226, 497–509. [https://doi.org/10.1016/s0021-9258\(18\)64849-5](https://doi.org/10.1016/s0021-9258(18)64849-5)
27. Wang, J., Li, M., Zheng, F., Niu, C., Liu, C., Li, Q., & Sun, J. (2018). Cell wall polysaccharides: Before and after autolysis of brewer's yeast. *World Journal of Microbiology and Biotechnology*, 34, 137. <https://doi.org/10.1007/s11274-018-2508-6>
28. Gu, Y., Lu, X., Liu, T., Song, Y., Sang, E., Ding, S., Liu, L., Xue, F., & Xu, P. (2023). Engineering the oleaginous yeast *Yarrowia lipolytica* to produce nutraceuticals: From metabolic design to industrial applications. *Food Bioengineering*, 2, 187–199. <https://doi.org/10.1002/fbe2.12062>
29. Bellou, S., Triantaphyllidou, I. E., Mizerakis, P., & Aggelis, G. (2016). High lipid accumulation in *Yarrowia lipolytica* cultivated under double limitation of nitrogen and magnesium. *Journal Of Biotechnology*, 234, 116–126. <https://doi.org/10.1016/j.jbiotec.2016.08.001>
30. Sestric, R., Spicer, V., V. Krokhin, O., Sparling, R., & B. Levin, D. (2021). Analysis of the *Yarrowia lipolytica* proteome reveals subtle variations in expression levels between lipogenic and non-lipogenic conditions. *FEMS Yeast Research*, 21, Article foab007. <https://doi.org/10.1093/femsyr/foab007>
31. Zhao, D., & Li, C. (2022). Multi-omics profiling reveals potential mechanisms of culture temperature modulating biosynthesis of carotenoids, lipids, and exopolysaccharides in oleaginous red yeast *Rhodotorula glutinis* ZHK. *Lwt*, 171, 114103. <https://doi.org/10.1016/j.lwt.2022.114103>
32. Wang, Y., Zhang, S., Zhu, Z., Shen, H., Lin, X., Jin, X., Jiao, X., & Zhao, Z. K. (2018). Systems analysis of phosphate-limitation-induced lipid accumulation by the oleaginous yeast *Rhodospiridium toruloides*. *Biotechnology for Biofuels*, 11, 148. <https://doi.org/10.1186/s13068-018-1134-8>
33. Wu, S., Zhao, X., Shen, H., Wang, Q., & Zhao, Z. K. (2011). Microbial lipid production by *Rhodospiridium toruloides* under sulfate-limited conditions. *Bioresource Technology*, 102, 1803–1807. <https://doi.org/10.1016/j.biortech.2010.09.033>

34. Zhao, Y., Song, B., Li, J., & Zhang, J. (2021). *Rhodotorula toruloides*: An ideal microbial cell factory to produce oleochemicals, carotenoids, and other products. *World Journal of Microbiology and Biotechnology*, 38, Article 13. <https://doi.org/10.1007/s11274-021-03201-4>
35. Hassan, T., Rahman, M. M., Rahman, M. A., & Nabi, M. N. (2022). Opportunities and challenges for the application of biodiesel as automotive fuel in the 21st century. *Biofuels Bioproducts & Biorefining-biofpr*, 16, 1353–1387. <https://doi.org/10.1002/bbb.2375>
36. Chebbi, H., Leiva-Candia, D., Carmona-Cabello, M., Jaouani, A., & Dorado, M. P. (2019). Biodiesel production from microbial oil provided by oleaginous yeasts from olive oil mill wastewater growing on industrial glycerol. *Industrial Crops and Products*, 139, Article 111535. <https://doi.org/10.1016/j.indcrop.2019.111535>
37. Gallego-García, M., Susmozas, A., Negro, M. J., & Moreno, A. D. (2023). Challenges and prospects of yeast-based microbial oil production within a biorefinery concept. *Microbial Cell Factories*, 22, 246. <https://doi.org/10.1186/s12934-023-02254-4>
38. Brakke, M. K. (1951). Density gradient centrifugation: A new separation technique. *Journal of the American Chemical Society*, 73, 1847–1848. <https://doi.org/10.1021/ja01148a508>
39. Bracero, V., Rosado, W., & Govind, N. S. (2014). Rapid procedure for separating high-lipid containing *Chlorella* sp. *Caribbean Journal of Science*, 48, 76–80. <https://doi.org/10.18475/cjos.v48i1.a1>
40. Liu, L., Pan, A., Spofford, C., Zhou, N., & Alper, H. S. (2015). An evolutionary metabolic engineering approach for enhancing lipogenesis in *Yarrowia lipolytica*. *Metabolic Engineering*, 29, 36–45. <https://doi.org/10.1016/j.ymben.2015.02.003>
41. Xu, J., Zhao, X., Wang, W., Du, W., & Liu, D. (2012). Microbial conversion of biodiesel byproduct glycerol to triacylglycerols by oleaginous yeast *Rhodospiridium toruloides* and the individual effect of some impurities on lipid production. *Biochemical Engineering Journal*, 65, 30–36. <https://doi.org/10.1016/j.bej.2012.04.003>
42. Bansal, N., Dasgupta, D., Hazra, S., Bhaskarm, T., Ray, A., & Ghosh, D. (2020). Effect of utilization of crude glycerol as substrate on fatty acid composition of an oleaginous yeast *Rhodotorula mucilagenosa* IIPL32: Assessment of nutritional indices. *Bioresource Technology*, 309, Article 123330. <https://doi.org/10.1016/j.biortech.2020.123330>
43. Galafassi, S., Cucchetti, D., Pizza, F., Franzosi, G., Bianchi, D., & Compagno, C. (2012). Lipid production for second generation biodiesel by the oleaginous yeast *Rhodotorula graminis*. *Bioresource Technology*, 111, 398–403. <https://doi.org/10.1016/j.biortech.2012.02.004>
44. Karamerou, E. E., Theodoropoulos, C., & Webb, C. (2017). Evaluating feeding strategies for microbial oil production from glycerol by *Rhodotorula glutinis*. *Engineering in Life Sciences*, 17, 314–324. <https://doi.org/10.1002/elsc.201600073>
45. Leiva-Candia, D. E., Tsakona, S., Kopsahelis, N., García, I. L., Papanikolaou, S., Dorado, M. P., & Koutinas, A. A. (2015). Biorefining of by-product streams from sunflower-based biodiesel production plants for integrated synthesis of microbial oil and value-added co-products. *Bioresource Technology*, 190, 57–65. <https://doi.org/10.1016/j.biortech.2015.03.114>
46. Uçkun Kiran, E., Trzcinski, A., & Webb, C. (2013). Microbial oil produced from biodiesel by-products could enhance overall production. *Bioresource Technology*, 129, 650–654. <https://doi.org/10.1016/j.biortech.2012.11.152>
47. Sriphuttha, C., Boontawan, P., Boonyanan, P., Ketudat-Cairns, M., & Boontawan, A. (2023). Simultaneous lipid and carotenoid production via *Rhodotorula paludigena* CM33 using crude glycerol as the main substrate: Pilot-scale experiments. *International Journal of Molecular Sciences*, 24, 17192. <https://doi.org/10.3390/ijms242417192>
48. Yen, H., Liu, Y., & Chang, J. (2015). The effects of feeding criteria on the growth of oleaginous yeast—*Rhodotorula glutinis* in a pilot-scale airlift bioreactor. *Journal of the Taiwan Institute of Chemical Engineers*, 49, 67–71. <https://doi.org/10.1016/j.jtice.2014.11.019>
49. Kamisaka, Y., Noda, N., Tomita, N., Kimura, K., Kodaki, T., & Hosaka, K. (2006). Identification of genes affecting lipid content using transposon mutagenesis in *Saccharomyces cerevisiae*. *Bioscience, Biotechnology, and Biochemistry*, 70, 646–653. <https://doi.org/10.1271/bbb.70.646>
50. Mussagy, C. U., Ribeiro, H. F., Santos-Ebinuma, V. C., Schuur, B., & Pereira, J. F. B. (2022). *Rhodotorula* sp.—based biorefinery: A source of valuable biomolecules. *Applied Microbiology and Biotechnology*, 106, 7431–7447. <https://doi.org/10.1007/s00253-022-12221-5>
51. Lin, P., Zhang, L. P., Du, G. C., Chen, J., Zhang, J., & Peng, Z. (2025). Construction of *Saccharomyces cerevisiae* platform strain for the biosynthesis of carotenoids and apocarotenoids. *Journal of Agricultural and Food Chemistry*, 73, 9187–9196. <https://doi.org/10.1021/acs.jafc.5c00088>
52. Khot, M., Raut, G., Ghosh, D., Alarcón-Vivero, M., Contreras, D., & Ravikumar, A. (2020). Lipid recovery from oleaginous yeasts: Perspectives and challenges for industrial applications. *Fuel*, 259, Article 116292. <https://doi.org/10.1016/j.fuel.2019.116292>

53. Kumar, L. R., Kaur, R., Tyagi, R. D., & Drogui, P. (2021). Identifying economical route for crude glycerol valorization: Biodiesel versus polyhydroxy-butyrate (PHB). *Bioresource Technology*, 323, Article 124565. <https://doi.org/10.1016/j.biortech.2020.124565>
54. Sun, H., Yang, M., Gao, Z., Wang, X., Wu, C., Wang, Q., & Gao, M. (2023). Economic and environmental evaluation for a closed loop of crude glycerol bioconversion to biodiesel. *Journal of Biotechnology*, 366, 65–71. <https://doi.org/10.1016/j.jbiotec.2023.03.001>

**Publisher's Note** Springer Nature remains neutral with regard to jurisdictional claims in published maps and institutional affiliations.

Springer Nature or its licensor (e.g. a society or other partner) holds exclusive rights to this article under a publishing agreement with the author(s) or other rightsholder(s); author self-archiving of the accepted manuscript version of this article is solely governed by the terms of such publishing agreement and applicable law.